

Brillouin scattering study of ferroelectric transition mechanism in multiferroic metal-organic frameworks of $[\text{NH}_4][\text{Mn}(\text{HCOO})_3]$ and $[\text{NH}_4][\text{Zn}(\text{HCOO})_3]$

Mirosaw Mczka, Maciej Ptak, and Seiji Kojima

Citation: *Applied Physics Letters* **104**, 222903 (2014); doi: 10.1063/1.4880815

View online: <http://dx.doi.org/10.1063/1.4880815>

View Table of Contents: <http://scitation.aip.org/content/aip/journal/apl/104/22?ver=pdfcov>

Published by the *AIP Publishing*

Articles you may be interested in

[Absence of ferroelectricity in \$\text{BiMnO}_3\$ ceramics](#)

J. Appl. Phys. **112**, 074112 (2012); 10.1063/1.4757944

[Terahertz and infrared studies of antiferroelectric phase transition in multiferroic \$\text{Bi}_{0.85}\text{Nd}_{0.15}\text{FeO}_3\$](#)

J. Appl. Phys. **110**, 074112 (2011); 10.1063/1.3650241

[Order-disorder behavior of ferroelectric phase transition of \$\text{KTa}_{1-x}\text{Nb}_x\text{O}_3\$ probed by Brillouin scattering](#)

Appl. Phys. Lett. **98**, 092909 (2011); 10.1063/1.3560345

[Micro-Brillouin scattering study of ferroelectric relaxor \$\text{Pb}\[\(\text{Zn}_{1/3}\text{Nb}_{2/3}\)_{0.91}\text{Ti}_{0.09}\]\text{O}_3\$ single crystals under the electric field along the \[001\] direction](#)

J. Appl. Phys. **98**, 044106 (2005); 10.1063/1.2008353

[Brillouin and dielectric studies of the phase transition in the relaxor ferroelectric \$\text{Pb}\(\text{Ni}_{1/3}\text{Nb}_{2/3}\)\text{O}_3\$](#)

J. Appl. Phys. **91**, 2262 (2002); 10.1063/1.1433183



AIP | Journal of
Applied Physics

Journal of Applied Physics is pleased to
announce **André Anders** as its new Editor-in-Chief

Brillouin scattering study of ferroelectric transition mechanism in multiferroic metal-organic frameworks of $[\text{NH}_4][\text{Mn}(\text{HCOO})_3]$ and $[\text{NH}_4][\text{Zn}(\text{HCOO})_3]$

Mirosław Maćzka,^{1,a)} Maciej Ptak,¹ and Seiji Kojima²

¹*Institute of Low Temperature and Structure Research, Polish Academy of Sciences, P.O. Box 1410, 50-950 Wrocław, Poland*

²*Institute of Materials Science, University of Tsukuba, Tsukuba, Ibaraki 305-8573, Japan*

(Received 17 April 2014; accepted 18 May 2014; published online 2 June 2014)

Temperature dependence of acoustic properties of $[\text{NH}_4][\text{Mn}(\text{HCOO})_3]$ and $[\text{NH}_4][\text{Zn}(\text{HCOO})_3]$ metal-organic frameworks was investigated by high-resolution micro-Brillouin scattering. Clear anomalies in the Brillouin shift and damping were observed near the transition temperature T_c upon cooling for the acoustic phonon corresponding to the c_{11} elastic constant. Analysis of the acoustic anomalies showed that the order parameter exhibits critical slowing down near T_c with the relaxation time of similar order of magnitude as for other order-disorder ferroelectrics. © 2014 AIP Publishing LLC. [<http://dx.doi.org/10.1063/1.4880815>]

Metal-organic frameworks (MOFs) have emerged as a promising class of compounds for various applications due to the huge number of organic ligands and metal ions combinations that offer the possibility of a systematic tuning of their physicochemical properties. Among these materials, metal-organic frameworks with formate ligands and divalent cations were shown in recent years to be a novel class of multiferroic materials with tailored magnetic and ferroelectric properties.^{1–4} $[\text{NH}_4][\text{Mn}(\text{HCOO})_3]$ (NH_4MnF) and $[\text{NH}_4][\text{Zn}(\text{HCOO})_3]$ (NH_4ZnF) belong to this family of hybrid organic-inorganic compounds exhibiting multiferroic properties. They undergo a ferroelectric phase transition at 254 and 191 K for NH_4MnF and NH_4ZnF , respectively, from the $P6_322$ to the $P6_3$ phase.⁴ It has been reported that this transition is associated with ordering of ammonium cations but detailed mechanism is still not well understood.⁴

In spite of great scientific and technological interests of MOFs, elastic properties of MOFs are poorly studied, especially as a function of temperature. Knowledge of elastic properties is, however, of great importance since they reflect the intrinsic interatomic bonding that governs the structure and stability of solids. In the family of $[\text{NH}_4][\text{M}(\text{HCOO})_3]$ compounds (M = divalent cation), Young's moduli measured by nanoindentation method were reported only for NH_4ZnF and only at room temperature.⁵ In the present Letter, we report the Brillouin scattering studies of NH_4MnF and NH_4ZnF in 113–343 and 93–303 K range, respectively, in order to understand the mechanisms of the phase transitions, and to find out whether these transitions are related to relaxation phenomena.

Single crystals were grown by a slow diffusion method reported elsewhere.⁴ The Brillouin spectra were obtained with a 3+3 pass tandem Sandercock-type Fabry-Perot interferometer combined with an optical microscope. The scattered light from the sample was collected in the back-scattering geometry. A cryostat cell (THMS 600) with a stability of 0.1 K was used for temperature variation.

Typical Brillouin spectra at selected temperatures corresponding to the acoustic phonons propagating along the x and z axes are shown in Fig. 1, where x and z correspond to the a and c hexagonal axes, respectively. A strong peak in Figs. 1(a) and 1(c) (1(b) and 1(d)) at about 22.4 and 24.5 GHz (30.1 and 32.2 GHz) for NH_4MnF and NH_4ZnF , respectively, correspond to the c_{11} (c_{33}) elastic constant. The weak peaks in Figs. 1(a) and 1(c) ($q\text{II}x$) at about 15.3 and 16.3 GHz (6.8 and 7.9 GHz) for NH_4MnF and NH_4ZnF , respectively, correspond to the c_{44} (c_{66}) elastic constant. Significantly different values of Brillouin shifts ν_∞ for longitudinal acoustic (LA) phonons propagating along the z and x axes reflect structural anisotropy of the framework. The ratio c_{33}/c_{11} is proportional to $(\nu_{33}/\nu_{11})^2$, and based on our data, it has been estimated as 1.81 and 1.73 for NH_4MnF and NH_4ZnF , respectively. This result points to slightly smaller elastic anisotropy of the Zn compound. It is worth noting that the decrease in elastic anisotropy for NH_4ZnF is correlated with decrease of the c/a ratio of the lattice parameters, which changes from 1.153 for NH_4MnF to 1.118 for NH_4ZnF . Since refractive indices of the studied crystals are not known, we cannot calculate the respective elastic constants. We may, however, estimate a ratio of elastic constants c_{ii} for NH_4MnF and NH_4ZnF . The ratio $c_{ii}^{\text{Zn}}/c_{ii}^{\text{Mn}} \approx (\rho^{\text{Zn}}/\rho^{\text{Mn}})(\nu_\infty^{\text{Zn}}/\nu_\infty^{\text{Mn}})^2$, where ρ denotes crystal density. Assuming the same refractive indices for the studied compounds, the ratio is about 1.32, 1.27, 1.26, and 1.49 for the c_{11} , c_{33} , c_{44} , and c_{66} elastic constants, respectively. This comparison shows that all elastic constants are significantly higher for NH_4ZnF , i.e., the stiffness of the structure increases when Mn^{2+} is replaced by smaller Zn^{2+} cation. This behavior is significantly different from that reported for the dimethylammonium Zn and Mn formates, i.e., for these compounds very similar Young's moduli were reported but the moduli increased for the Co and Ni analogues.⁶ It has been argued that there is a correlation between elastic modulus and ligand field stabilization energy (LFSE), i.e., mechanical stability increases with greater LFSE.⁶ Our result shows that this conclusion is not valid in the ammonium

^{a)}Author to whom correspondence should be addressed. Electronic mail: m.maczka@int.pan.wroc.pl

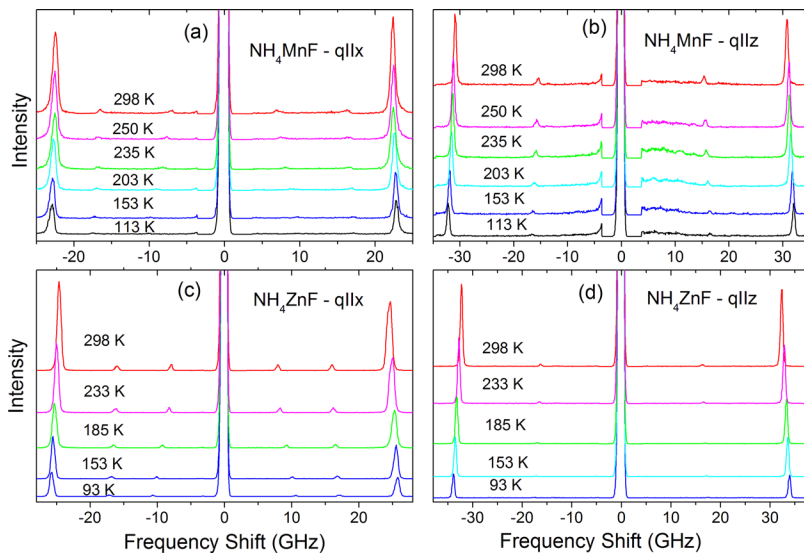


FIG. 1. Representative Brillouin spectra of NH_4MnF ((a) and (b)) and NH_4ZnF ((c) and (d)) at selected temperatures corresponding to the acoustic phonons propagating along the x - and z -axis.

compounds studied here, since they differ significantly in the mechanical stability in spite of zero LFSE.

The plots of frequency versus temperature for LA modes traveling along the z axis show no anomaly for NH_4MnF and very weak, smooth growth near T_c for NH_4ZnF (see Fig. 2). The transverse acoustic (TA) modes show nearly linear temperature dependence down to T_c followed by significant growth below T_c . Very similar shapes of the acoustic anomalies near T_c are also observed for the TA modes traveling along the x axis (see Fig. 3). Such anomalies of the TA modes are characteristic for the biquadratic coupling between the order parameter η and corresponding strain components ε of the type $\varepsilon^2\eta^2$. Fig. 3 also shows that frequency of the LA mode traveling along the x axis exhibits very weak downward step near T_c for NH_4ZnF . The observation of downward step indicates that this LA mode couples with square of the order parameter. This step-like anomaly starts at about 190 K and the minimum frequency occurs at about 187 K. This mode also exhibit distinct anomaly in the temperature dependence of full width at half maximum (FWHM) with maximum at about 188 K. More pronounced downward step and FWHM anomaly for the discussed LA mode is observed for NH_4MnF while other acoustic phonons

do not show any anomalies in FWHM. In this case, the step starts at about 249 K and the minimum frequency is at 238 K while FWHM is maximum at about 241 K. As can be noticed, the observed softening at 190 K for NH_4ZnF agrees well with $T_c = 191$ K but for NH_4MnF this downward step starts at about 5 K lower temperature than T_c . This difference can be most likely attributed to some temperature gradient in the sample and presence of some defects. Another interesting observation is that the downward step is not very sharp, especially for the NH_4MnF compound, for which it extends over 11 K. Moreover, the maximum value of FWHM is located almost in the middle of the step. Such behavior suggests that the observed step-like frequency changes are associated with an order-disorder transition at T_c .

Let us now discuss the acoustic properties in the framework of Landau theory. The driving order parameter of the $P6_322$ to $P6_3$ phase transition in the studied compounds is associated with the critical wave vector $\mathbf{K2}$ of the paraelectric phase.⁷ The transition is induced by freezing of the η_1 component of the order parameter and the corresponding free energy expansion takes the form:

$$F = a_1(\varepsilon_1 + \varepsilon_2)\eta_1^2 + a_3\varepsilon_3\eta_1^2 + a_4(\varepsilon_4^2 + \varepsilon_5^2)\eta_1^2 + a_5[(\varepsilon_1 - \varepsilon_2)^2 + \varepsilon_6^2]\eta_1^2, \quad (1)$$

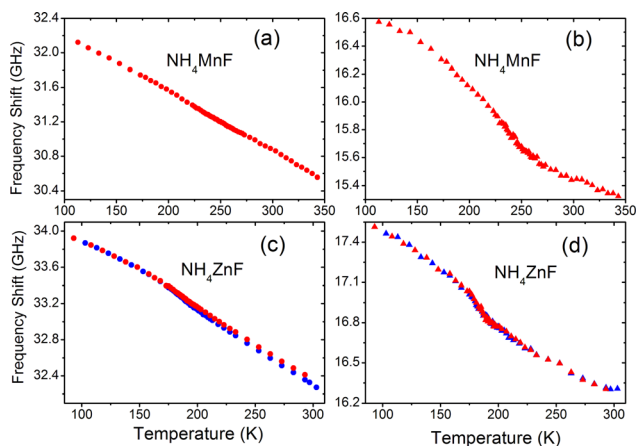


FIG. 2. Temperature dependence of frequency shift for LA ((a) and (c)) and TA phonons ((b) and (d)) propagating along the z axis. Blue and red color correspond to cooling and heating run, respectively.

where a_1 , a_3 , a_4 , and a_5 denote coupling constants. Detailed analysis presented by Carpenter *et al.* showed that in the static approximation, the c_{33} elastic constant should exhibit step-like frequency change, the c_{44} and c_{66} elastic constants should increase above T_c by $2a_4\eta_1^2$ and $2a_5\eta_1^2$, and $c_{11} = c_{22}$ should have two contributions: step-like decrease and increase proportional to $2a_5\eta_1^2$.⁷ As mentioned above, the observed acoustic anomalies are consistent with the expected changes but they also suggest additional contribution due to dynamic effects.

It is well-known that the fluctuation of electric polarization ΔP shows a characteristic anisotropy near T_c owing to the long range electrostatic dipole-dipole interaction.^{8,9} The longitudinal component of ΔP is suppressed by the appearance of the depolarization field, while the transverse one is not. As a result, if a phonon propagates along the direction

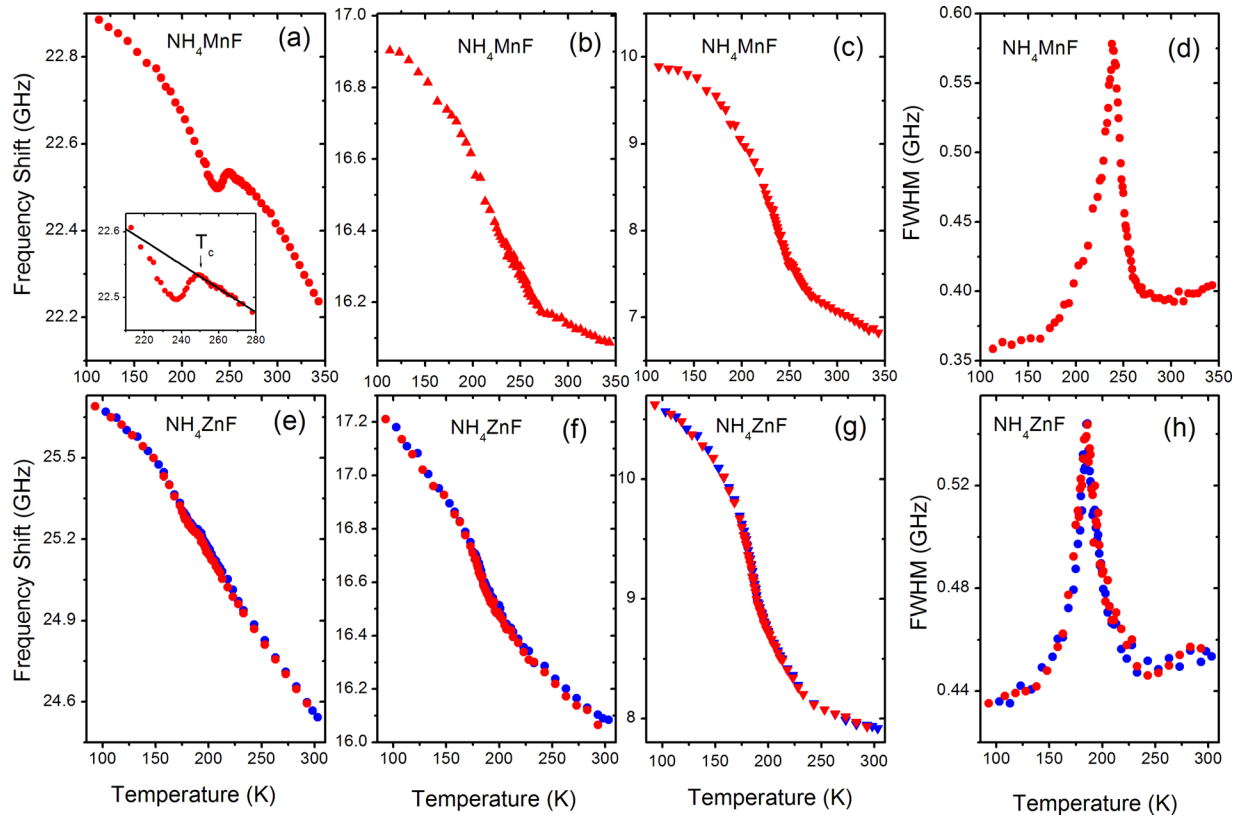


FIG. 3. Temperature dependence of frequency shift for LA ((a) and (e)) and TA phonons ((b), (c), (f), and (g)) propagating along the x axis. (d) and (h) show temperature dependence of FWHM for LA phonons propagating along the x axis. Blue and red colors correspond to cooling and heating run, respectively. Inset in (a) shows details of the acoustic anomaly and the solid line corresponds to the fit of the experimental data in the 250–278 K range to a linear function.

parallel to polarization, Brillouin spectra usually do not show any anomaly in FWHM because of the suppressed fluctuation. If a phonon propagates perpendicular to polarization, strong anomaly is predicted to be observed.^{10,11} In the family of $[\text{NH}_4][\text{M}(\text{HCOO})_3]$ compounds, spontaneous polarization appears along the z axis.^{4,12} Thus, the observed lack of any anomaly for the LA mode propagating along the z axis seems to be consistent with the depolarization field effect. It is worth noting, however, that some anomalous broadening of the LA mode propagating along the x axis is also observed above T_c . This additional broadening, not observed for the LA mode propagating along z axis, cannot be explained by the depolarization field effect since there is no P_s in the paraelectric phase. We suppose that this contribution comes from a local piezoelectric coupling inside precursor polar clusters with local point symmetry C_6 . For the ferroelectric point group 6, the relevant piezoelectric constants are $d_{31} = d_{32}$ and d_{33} . When d_{33} constant is much smaller than $d_{31} = d_{32}$, the phonon traveling along the z axis may show no anomaly.

The observed acoustic anomaly can be analyzed to obtain information on the relaxation time τ_{LA} by the LA phonon in the ferroelectric phase. Assuming that the single relaxation time is appropriate, it can be determined from the relation¹³

$$\frac{1}{2\pi\tau} = \frac{\nu_\infty^2 - \nu_0^2}{\Gamma_0 - \Gamma_\infty}. \quad (2)$$

Here, ν_∞ (Γ_∞) is the observed Brillouin shift (FWHM) and ν_0 (Γ_0) is the Brillouin shift (FWHM) not affected by the

transition. The FWHM observed far above T_c (0.4 GHz) was taken as Γ_0 . In order to evaluate ν_0 , data in the 250–278 K range were fitted by a linear ν_0 . The plot of $1/\tau$ obtained from the experimental data for the c_{11} mode of NH_4MnF with the help of Eq. (2) is shown in Fig. 4. As it can be seen, $1/\tau$ is approximately a linear function of temperature. Such behavior is known as a critical slowing down, where $1/\tau_{\text{LA}}$ can be described by the formula¹⁴

$$\frac{1}{\tau_{\text{LA}}} = \frac{T_c - T}{T_c} \frac{1}{\tau_1}. \quad (3)$$

The best fit to the experimental data with Eq. (3) yields $\tau_1 = 0.46$ ps. The relaxation time in the ferroelectric phase of

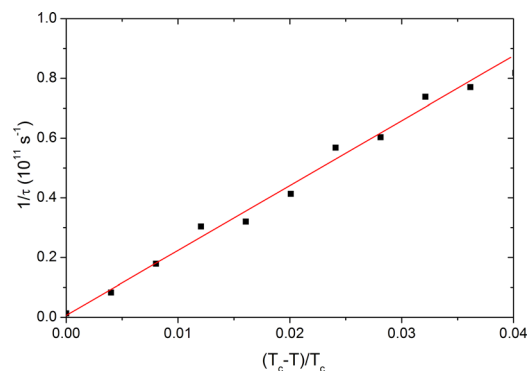


FIG. 4. Temperature dependence of inverse relaxation time $1/\tau$ estimated from temperature dependence of the LA phonon of NH_4MnF propagating along the x axis.

NH_4MnF is of similar order of magnitude as the relaxation times observed for typical order-disorder ferroelectrics, for instance, KH_2PO_4 with $\tau_1 = 0.12$ ps.¹⁵

In an order-disorder phase transition, a softening of an elastic constant, in respect to the static value, will be observed at sufficiently low frequency ω , so that $\omega\tau \ll 1$, whereas for slow relaxation times and high frequency ($\omega\tau \gg 1$) an elastic constant should not exhibit any softening.¹⁶ The plausible explanation of significantly weaker anomalies for the LA mode propagating along the x axis for NH_4ZnF when compared to NH_4MnF is slower relaxation of the polarization in the former case and/or weaker smaller coupling constant between the LA mode and the polarization fluctuation. Since in the ammonium and amine templated metal formate frameworks the organic cation was shown to be the main source of electric polarization,¹⁷ the observed behavior can be most likely attributed to a tighter binding of the NH_4^+ cations in the Zn-formate framework than in the Mn-formate framework.

In conclusion, our results indicate that the stiffness of the structure increases when Mn^{2+} is replaced by smaller Zn^{2+} cation. They also confirm the ferroelectric nature of the structural phase transition in ammonium metal formates and reveal critical slowing down of the order parameter near T_c for NH_4MnF .

This research was supported by the National Center for Science (NCN) in Poland under Project No.

DEC-2011/03/B/ST5/01019. M. Maczka acknowledges Dr. Tae Hyun Kim for technical help in Brillouin measurements.

¹R. Ramesh, *Nature* **461**, 1218 (2009).

²G. Rogez, N. Viart, and M. Drillon, *Angew. Chem., Int. Ed.* **49**, 1921 (2010).

³P. Jain, V. Ramachandran, R. J. Clark, H. D. Zhou, B. H. Toby, N. S. Dalal, H. W. Kroto, and A. K. Cheetham, *J. Am. Chem. Soc.* **131**, 13625 (2009).

⁴G. C. Xu, W. Zhang, X. M. Ma, Y. H. Chen, L. Zhang, H. L. Cai, Z. M. Wang, R. G. Xiong, and S. Gao, *J. Am. Chem. Soc.* **133**, 14948 (2011).

⁵W. Li, M. R. Probert, M. Kosa, T. B. Bennett, A. Thirumurugan, R. P. Burwood, M. Parinello, J. A. K. Howard, and A. K. Cheetham, *J. Am. Chem. Soc.* **134**, 11940 (2012).

⁶J. C. Tan, P. Jain, and A. K. Cheetham, *Dalton Trans.* **41**, 3949 (2012).

⁷M. A. Carpenter, C. J. Howard, M. J. Andrew, R. E. A. McKnight, Y. Liu, and R. L. Withers, *J. Appl. Phys.* **107**, 013505 (2010).

⁸A. Aharony, *Phys. Rev. B* **8**, 3363 (1973).

⁹M. Tokunaga, *Prog. Theor. Phys.* **51**, 1002 (1974).

¹⁰T. Yagi, *Ferroelectrics* **150**, 131 (1993).

¹¹T. Yagi, M. Tokunaga, and I. Tatsuzaki, *J. Phys. Soc. Jpn.* **40**, 1659 (1976).

¹²M. Maczka, A. Pietraszko, B. Macalik, and K. Hermanowicz, *Inorg. Chem.* **53**, 787 (2014).

¹³W. Rehwald, *Adv. Phys.* **22**, 721 (1973).

¹⁴M. E. Lines and A. M. Glass, *Principles and Application of Ferroelectrics and Related Materials* (Clarendon, Oxford, 1977), Chap. 8, p. 241.

¹⁵I. Tatsuzaki, M. Kasahra, M. Tokunaga, and H. Tanaka, *Ferroelectrics* **39**, 1049 (1981).

¹⁶H. Z. Cummins, in *Light Scattering Near Phase Transitions* edited by H. Z. Cummins and A. P. Levanyuk (North-Holland, Amsterdam, 1983).

¹⁷D. Di Sante, A. Stroppa, P. Jain, and S. Picozzi, *J. Am. Chem. Soc.* **135**, 18126 (2013).